THE ASTROPHYSICAL JOURNAL, 273:44–57, 1983 October 1

A SINGLE EXHAUST MODEL FOR BACKWARD EMISSION IN DOPPLER QUASARS

J. V. NARLIKAR AND K. SUBRAMANIAN
Tata Institute of Fundamental Research
Received 1982 November 19; accepted 1983 March 8

ABSTRACT

This paper provides an astrophysical scenario for Hoyle's conjecture that quasars ejected at high velocities from active galactic nuclei radiate predominantly in a narrow backward cone. Backward emission is essential in a local Doppler theory in order to explain why no blueshifted quasars are seen.

The mechanism suggested here is an adaptation of the twin exhaust model of Blandford and Rees. It is argued that a fast moving quasar encounters a strong ram pressure from the intergalactic medium in the forward direction which suppresses the forward exhaust. By contrast, the only exhaust from the object is along the line of least resistance lying in the backward direction.

The model has several constraints from hydrodynamics, gravitation theory, and radiation requirements as well as the primary motivation that no blueshifted quasars are seen. It is shown that the model survives these constraints for a comfortable range of parameters and helps in understanding some of the observable properties of quasars.

Subject headings: galaxies: jets — quasars — radiation mechanisms

I. INTRODUCTION

The idea that quasars derive their large redshifts from Doppler effect has been in the literature from the early days of their discovery. The first suggestion came from Terrell (1964) that quasars were ejected from the nucleus of our Galaxy. This idea would be hard to sustain in view of the manifestly nonactive nature of the galactic nucleus. A later suggestion by Hoyle and Burbidge (1966) advocated active galactic nuclei as possible sources of ejection. From observations of quasar-galaxy associations and quasar-quasar associations Arp (1967, 1977) has argued in favour of quasars being ejected from galaxies.

Such ideas represent the minority view in the redshift controversy concerning quasars, the majority taking it for granted that these redshifts are due to the expansion of the universe. We do not wish to discuss the various arguments advanced in support of the opposing views in this controversy (see, for example, Field, Arp, and Bahcall 1973; Burbidge 1973, 1979; and Rees 1977). Rather we concentrate here on the major drawback of the Doppler hypothesis, a drawback which will be referred to as the *blueshift catastrophe.*

The blueshift catastrophe was first expressed quantitatively by Strittmatter (1967) as follows. Suppose all quasars are equally bright intrinsically, radiate isotropically in their rest frames with a spectrum $\propto \nu^{-\alpha}$ (ν = frequency, α = spectral index), and are being ejected isotropically by sources distributed uniformly around the observer. Then in a flux limited sample, the number of blueshifted quasars N_b is related to the number of redshifted quasars N_r by the ratio

$$\frac{N_b}{N_r} = (1 + z_{\max})^{3+\alpha}, \tag{1}$$

$z_{\max}$ being the maximum redshift observed in the sample. With $z_{\max} = 2$, $\alpha = 1$, Strittmatter had estimated this ratio to be as high as 81. Since larger redshifts are known now, the ratio could be even higher. Why are no blueshifted quasars seen to date?

Hoyle (1980) suggested a resolution of the blueshift catastrophe by arguing that quasars emit preferentially backwards. If a Doppler shifted quasar of speed V relative to an observer radiated only with a backward cone of semivertical angle

$$\theta_H = \cos^{-1} \frac{c - (c^2 - V^2)^{1/2}}{V} \tag{2}$$

in its rest frame, then the observer will not see the quasar blueshifted. In an earlier paper (Narlikar and Subramanian 1982, hereafter Paper I) we had discussed the various kinematical and dynamical implications of this idea. We had shown that a significant damping of radiation outside the Hoyle angle θ_H was consistent with the observations of aligned triplets of quasars observed by Arp and Hazard (1980) and by Saslaw (as quoted by

Arp and Hazard 1980). We also showed that the ratio $N_b:N_r$ becomes as small as a few percent, once predominantly backward radiation is assumed.

Why should a quasar emit radiation anisotropically in its rest frame? This question was not considered by us in Paper I. The model of anisotropic emission given there was empirical, and it was used to establish a prima facie case on observational grounds. In the present paper we give an astrophysical answer to the above question. Although the model discussed by us arose from the Doppler shift hypothesis, it may be able to account for some of the morphological features of quasars whether they are local or distant.

II. SCENARIOS FOR BACKWARD EMISSION

Although Hoyle (1980) was the first to lay down explicit requirements in terms of the Hoyle angle, the importance of backward emission for the avoidance of blueshift catastrophe was appreciated even earlier by Strittmatter (1967) who tried, without success, several scenarios for this purpose. Our initial experience was similar, although we now feel that we finally have a working model.

Note first that a quasar moving at high velocity through the intergalactic medium (IGM) does have an inherent anisotropy in its rest frame. This is so because in its rest frame the IGM is flowing toward it at relativistic speed. The question is, in what way (if any) would this anisotropy influence the emission pattern of radiation from the object.

It was suggested by Hoyle (1980) that the IGM would tend to pile up in front of the quasar while in its rear the medium would be rarefied. This process would increase the opacity and reduce the radiation in the forward direction while facilitating the backward emission.

A second possibility is suggested by accretion. A moving mass would accrete matter from the surroundings leading to a concentration in its wake. Such piled up matter in the back might radiate (Ruderman and Spiegel 1971). Neither of these ideas, however, works when considered quantitatively.

The third possibility is based on the adaptation of the twin exhaust model of Blandford and Rees (1974, hereafter BR). In the original BR model, we have a rotating massive object made of star systems surrounded by gas in which an energy machine at the center pours out hot plasma. Although initially expanding isotropically, the plasma quickly selects the directions of least resistance which are along the axis of rotation. The plasma is therefore squirted out in well-collimated fashion along opposite directions lying on the rotation axis.

In our adaptation of this idea, we will argue that for a fast moving quasar, there is an appreciable ram pressure from the IGM in the forward direction. The line of least resistance for outward moving plasma is along the backward direction. Thus one de Laval nozzle is formed in the backward direction. The bulk of the quasar's continuum radiation is emitted by the plasma in the nozzle in the backward direction due to relativistic beaming. The line radiation from cooler clouds in the squirted plasma is blocked in the forward direction by the dust in the object itself, while it escapes relatively undisturbed in the backward direction. Figure 1 illustrates the general scenario.

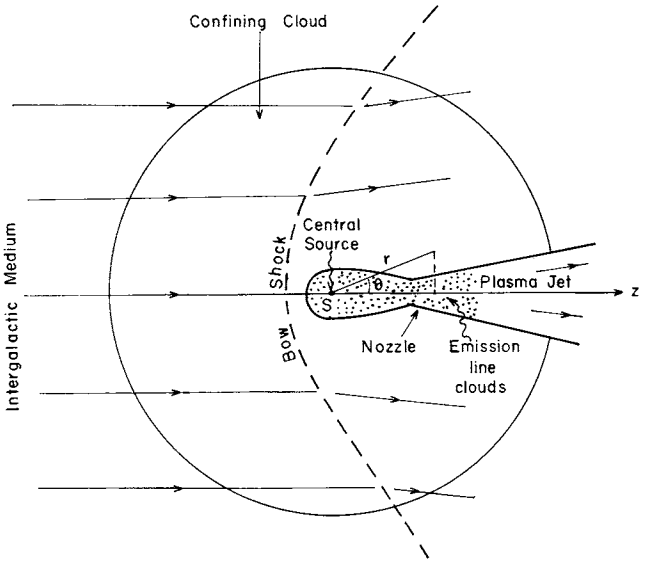

FIG. 1.—The components of the proposed quasar model in the rest frame of the quasar. The figure also illustrates the formation of a single backward jet when the intergalactic medium flows through the gas cloud as in case A. The polar coordinates (r, θ) are measured from the central source with $\theta = 0$ the backward direction.

The rest of this paper will be concerned with working out the quantitative details of this model. There are several constraints which have to be taken into account. In § III we consider the gasdynamic constraints, such as the survival of the enveloping gas cloud as it moves rapidly through the IGM, the pressure distribution which permits the formation of a jet and the circumstances under which the forward jet is blocked. In § IV we discuss how the BR parameters can be adapted and scaled down for local quasars. In § V we outline the requirements of continuum emission, its magnitude and anisotropy. In § VI we investigate the constraints on line emission and the resolution of the blueshift catastrophe.

It will be seen that in spite of the many checks the model survives with a comfortable range of parameters. In § VII we discuss some of its observable implications and also suggest that some features of the model can be retained irrespective of whether the quasars are local objects.

III. GASDYNAMICS OF THE SINGLE EXHAUST MODEL

a) *The Model Components, Types, and Cases*

As mentioned in § II our model consists of three components: (*i*) a central source of hot plasma, (*ii*) a cloud of gas and dust surrounding the central source, and (*iii*) a matter distribution whose gravity holds the cloud together. Since it is assumed that quasars are ejected from nuclei of galaxies, the composition of these objects should broadly resemble what is believed to exist in active galactic nuclei. Our quasars are, however, scaled-down versions of the objects considered by BR, because in a local hypothesis the requirements of mass and luminosity are scaled down. We will adopt the general notation that if a physical quantity has the magnitude Q_n in certain units, then its actual value measured in those units is $Q_n \times 10^n$. The exceptions to this rule will be clear from the context, e.g., $r_{\rm pc}$ will denote the measure of r in parsecs.

The matter distribution to be considered will be of two types. Type I denotes a uniform density distribution like the star cluster assumed by BR. Such a distribution produces a flat-bottomed well of gravitational potential. Type II corresponds to a collapsed massive object of radius $r^{(s)}$ which produces a cusplike potential.

Unless otherwise stated we will work in the rest frame of the quasar. There by "forward" direction we mean the direction in which the quasar is heading as seen by the observer. With this teminology, the quasar sees the IGM moving in the "backward" direction.

Since the flow velocity V of the IGM is relativistic, it will be supersonic, and hence we have to consider whether a bow shock will form in front of the quasar. For a cloud with nucleon number density $n^{(c)}$, collision cross section σ, and typical cloud size $l^{(c)}$, an IGM particle will have a collision only if

$$n^{(c)}\sigma l^{(c)} > 1 . \tag{3}$$

For the relevant range of parameters discussed in § IV, the inequality (3) will not be satisfied. In this case the IGM just flows through the cloud without generating a shock. We will refer to this as case A. If, however, magnetic fields are also present in the vicinity of the gas cloud, collisionless shocks can form. Case B assumes the formation of a bow shock in front of the objects.

b) *The Fate of the Gas Cloud under the Onslaught of IGM*

The first question that needs to be answered is whether the gas cloud is swept away by the fast moving IGM. A negative answer, necessary for the working of the model, requires a sufficiently strong gravitational binding. We estimate this requirement for the cases A and B.

Case A.—Assuming that a typical particle in the cloud or the IGM has mass equal to the proton mass m_p, the sweeping force exerted by the IGM will be $\sim n^{(c)}n^{(I)}\sigma m_p \gamma^2 V^2$ per unit volume, where $\gamma = [1 - (v^2/c^2)]^{-1/2}$. This force must be less than the gravitational force exerted on a typical fluid element in the cloud by the mass distribution. In type II, for a central massive object of mass M this requirement at a distance $r > r^{(s)}$ from the center becomes

$$\frac{GMm_p n^{(c)}}{r^2} > n^{(c)}n^{(I)}\sigma m_p c^2(\gamma^2 - 1) . \tag{4}$$

We denote by $R^{(c)}$ the value of r at which the two terms become equal. A cloud of radius exceeding $R^{(c)}$ will be disrupted by the IGM. The inequality (4) is the first of the numerous constraints on the model. A similar condition can be written down for type I.

Case B.—This case has been discussed by others in different contexts. See, for example, the discussion of head-tail sources by Jones and Owen (1979) and Henriksen, Vallée, and Bridle (1981) and of sweeping of gas from galaxies by the intracluster medium by Lea and De Young (1976). The presence of the shock leads to transient effects which persist for the sound travel time across the cloud. After the transient effects have died down, the whole system feels the full ram pressure force. We will consider these two stages separately.

The transient pressure gradient in the cloud is of the order of $n^{(I)}m_p c^2(\gamma^2 - 1)/r$, where r is the radius of the cloud. Replacing the right-hand side of inequality (4) by this quantity we get the inequality (for type II)

$$\frac{GMn^{(c)}}{rn^{(I)}c^2(\gamma^2 - 1)} > 1 . \tag{5}$$

The transient effect will persist for the sound travel time across the cloud. We now derive the inequality corresponding to expression (5), imposed under the steady conditions after the transient effects have died down.

If g is the effective deceleration produced by the ram pressure, then $n^{(c)}m_p g$ is the corresponding force per unit volume of the cloud. The ram pressure $\sim n^{(I)}m_p V^2\gamma^2$ acting on a cross section of the order Ar^2, where r is cloud radius and A is a dimensionless constant of order unity, would produce a force $Ar^2n^{(I)}m_p c^2(\gamma^2 - 1)$. Dividing this by mass M we get an estimate of g. Comparing the ram pressure force with the gravitational binding we get

$$\frac{GM^2}{An^{(I)}m_p c^2(\gamma^2 - 1)r^4} > 1 . \tag{6}$$

For the parameters chosen in § IV the inequality (6) is less stringent than inequality (5) so that if the cloud survived the transient effects, it would survive the steady conditions thereafter. These considerations apply to type I models also, without any significant modification.

c) *The Pressure Distribution of the Cloud*

Our eventual aim is to study the formation of the backward jet, and for this purpose we need to know the pressure distribution in the ambient cloud. We will assume that the model parameters are such that the cloud remains intact in spite of the bombardment from the IGM. The internal equilibrium of the cloud is given by the hydrostatic equation

$$\nabla p = -\rho\nabla\phi + \boldsymbol{F} , \tag{7}$$

where p is the pressure, ρ, the gas density, and ϕ, the gravitational potential. We will assume that the self-gravity of the cloud is negligible compared to the force exerted by the mass M. $\boldsymbol{F}$ is the external force per unit volume.

If $\boldsymbol{F} = 0$, for type I distribution (7) gives the integral obtained by BR,

$$p = p_0 \exp\left(-\frac{r^2}{K^2}\right), \qquad p_0 = \text{constant} , \tag{8}$$

where

$$K = \frac{\pi G\rho^{(s)}m_p}{3kT} . \tag{9}$$

Here $\rho^{(s)}$ is the (uniform) matter density, and the cloud is taken to be at a uniform temperature T. For type II the integral in the case $\boldsymbol{F} = 0$ is

$$p = p_s \exp\left[l\left(\frac{1}{r} - \frac{1}{r^{(s)}}\right)\right], \tag{10}$$

where p_s is the pressure at $r = r^{(s)}$, and

$$l = \frac{GMm_p}{2kT} . \tag{11}$$

A combination of equations (8) and (10) applies if we assume that the uniform distribution of type I extends to $r = R^{(s)}$, where $R^{(s)}$ is less than the cloud radius. Then the pressure in the cloud at $r < R^{(s)}$ is given by

$$p(r) = p_0 \exp\left[-\frac{R^{(s)2}}{K^2} + l\left(\frac{1}{r} - \frac{1}{R^{(s)}}\right)\right] . \tag{12}$$

Consider how these formulae are modified if the IGM is flowing past the object. In case A, the IGM flows through the cloud exerting a force

$$\boldsymbol{F} = n^{(I)}\sigma\rho v^2\gamma^2\hat{\boldsymbol{z}} , \tag{13}$$

where $\hat{\boldsymbol{z}}$ is a unit vector in the direction of flow of the IGM in the quasar's rest frame (i.e., the backward direction). For an isothermal cloud, we may write $\rho = pm_p/2kT$.

Writing $R = r \sin \theta$, $z = r \cos \theta$, we get the following solution of equation (7) in type I model:

$$p = p_0 \exp\left(-\frac{r^2}{K^2} + \frac{r \cos \theta}{K_A}\right), \tag{14}$$

where

$$K_A = \frac{2kT}{n^{(I)} m_p \sigma c^2 (\gamma^2 - 1)}. \tag{15}$$

Similar equations can be set up for matter distribution of type II and the pressure calculated.

In case B, the transient effects will be important when we consider the formation of the jet, but once the jet is formed, its parameters will be eventually governed by the steady state conditions. In steady state the ram pressure tends to accelerate the gas. From considerations of § IIIb, we can express this effect as that of a negative force in the equilibrium equation (7), i.e., by $\boldsymbol{F} = -\rho A n^{(I)} r^{(c)2} m_p c^2 (\gamma^2 - 1)\hat{\boldsymbol{z}}/M$, where $r^{(c)}$ is the cloud radius. The resulting solution of the gasdynamic equations would be similar to that in case A for both types. The constant K_A will be replaced by

$$K_B = \frac{2kTM}{A n^{(I)} r^{(c)2} m_p c^2 (\gamma^2 - 1)}, \tag{16}$$

and the cos θ term will appear with the opposite sign.

Putting numbers into expressions (9), (11), (15), and (16) we find that for the model parameters derived in § IV,

$$\frac{K}{K_A} \ll 1, \quad \frac{K}{K_B} \ll 1, \quad \left(\frac{l}{K_A}\right)^{1/2} \ll 1, \quad \left(\frac{l}{K_B}\right)^{1/2} \ll 1. \tag{17}$$

In other words, the IGM does not introduce significant distortion into the internal structure of the cloud.

d) Formation of a Single Backward Jet

Although the IGM does not blow away or distort the surrounding gas cloud, it plays an important role in controlling the structure of the jet issuing from the central region. In the absence of detailed numerical computations, our discussion will be somewhat simplistic but sufficient to establish that the model works. As in our earlier discussions we consider case A and case B separately.

Case A.—We assume that the central source in the object ejects hot plasma isotropically to start with. However, the expanding sphere of plasma encounters uneven pressure from the surroundings, because of the incoming IGM; the pressure from IGM being maximum and equal to $P^{(I)} \sim n^{(I)} m_p c^2 (\gamma^2 - 1)$ in the forward direction and zero in the backward direction. The actual sequence of events that leads to the "feel" of the pressure in the forward direction would be something like the following.

The plasma would have magnetic fields which would stop the incoming IGM through a collisionless shock. The plasma then feels the above pressure and begins to decelerate. In the forward off-axis position if ϕ is the angle between the normal to the plasma surface and the forward direction, then this pressure is reduced to a fraction $\cos^2 \phi$ of its value at $\phi = 0$.

In the backward direction this pressure helps rather than hinders the plasma flow. If $P^{(I)}$ is comparable to p_0 or p_s (depending on type I or II), then the pressure hill in the forward direction will cause the plasma to seek the least resistant direction for outlet, which is in the backward direction. Situations like this have been discussed in the context of single jet models by Wiita and Siah (1982) and also commented on by Icke (1983). In the present picture, the plasma breaches the confining cloud in the backward direction giving rise to a rarefaction wave. This wave further helps in stopping the expansion in other directions which the IGM ram pressure is already doing. Thus, a single backward jet results.

After the steady state has been established, there will be a bow shock standing off the forward portion of the jet as shown in Figure 1. This will not affect our previous conclusion of § IIIc concerning the negligible effect of the IGM on the cloud, for the effects of a shock are that it leaves behind an increased thermal pressure, an increased particle number density, and a decreased velocity of the shocked gas. The extra pressure is significant only in the forward direction where we have already taken it into account while considering the formation of the jet. Its effect in the off-axis direction falls off as $\cos^2 \phi$ and is negligible at the back. Further, as the gas in IGM passes through the shock, V decreases while $n^{(I)} V \gamma$ remains constant because of flux conservation. Hence $n^{(I)} V^2 \gamma^2$ decreases, and our inequality (4) was more stringent than necessary. For the same reasons the pressure distribution in the cloud will be affected to a lesser extent than calculated in § IIIc.

Case B.—Here the transient effects which last for $\sim 10^4$ yr in typical cases are likely to be important in the early stages of jet formation. As the plasma from the center begins to expand, transient pressure gradients begin to act against the plasma expansion in the forward direction while they tend to accelerate the expansion in the backward direction. The sequence of events leading to the formation of a jet is similar to that for case A.

After the transient effects are over, it is natural to expect the plasma to keep flowing along the backward direction along the channel scooped out by the jet initially. BR had argued that a single jet is unstable and that another jet in the opposite direction soon develops. In our scenario, however, this cannot happen, for a forward jet emerging from the cloud will once again be opposed by the ram pressure of the IGM which has already been shocked by the cloud. The forward jet is slowed down and eventually stopped. A compression wave may develop due to the piling of the plasma in the slowed down jet. This wave will travel in the backward direction and enhance the effect of the ram pressure from the IGM. Once again, the result is the sealing of the forward jet and continuation of the backward one. The steady configuration is illustrated in Figure 2.

IV. PARAMETERS OF THE MODEL

We now follow the BR analysis for working out the numerical values of the parameters of our model illustrated in Figures 3*a* and 3*b*. Arguments given so far require the ram pressure $P^{(I)}$ to be of the same order as p_0 (for type I) or p_s (for type II) in order that a single backward jet is created and sustained. We shall accordingly write the central pressure in the cloud to be of the order

$$P^{(I)} = n^{(I)} m_p c^2 (\gamma^2 - 1)$$
$$\approx 1.5 \times 10^{-8} n_{-5}^{(I)} (\gamma^2 - 1) . \quad (18)$$

We have assumed here that $n^{(I)} \sim 10^{-5}$ cm^{-3}. There is growing evidence for the existence of intracluster gas of density 10^{-3} to 10^{-4} cm^{-3} at temperatures of $\sim 10^8$ K (Field 1972; Fabian and Kembhavi 1982). If quasars are ejected from galaxies in a cluster, then $n^{(I)}$ will be somewhat higher than 10^{-5} cm^{-3}. BR have suggested values as high as 10^{-2} cm^{-3} in their discussion of radio sources in clusters of galaxies.

In a typical "local" quasar the luminosity may be in the range $\sim 10^{40}$–10^{42} ergs s^{-1} (corresponding to a range of 10^{44}–10^{46} ergs s^{-1} in the cosmological hypothesis). We will accordingly express the luminosity by L_{41} in units of 10^{41} ergs s^{-1}. The BR analysis (cf. the Appendix of their paper) gives the nozzle radius in terms of the central pressure and luminosity by the formula

$$l^* = \left(\frac{3\sqrt{3}}{8\pi}\right)^{1/2} \left(\frac{L}{p_0 c}\right)^{1/2} . \quad (19)$$

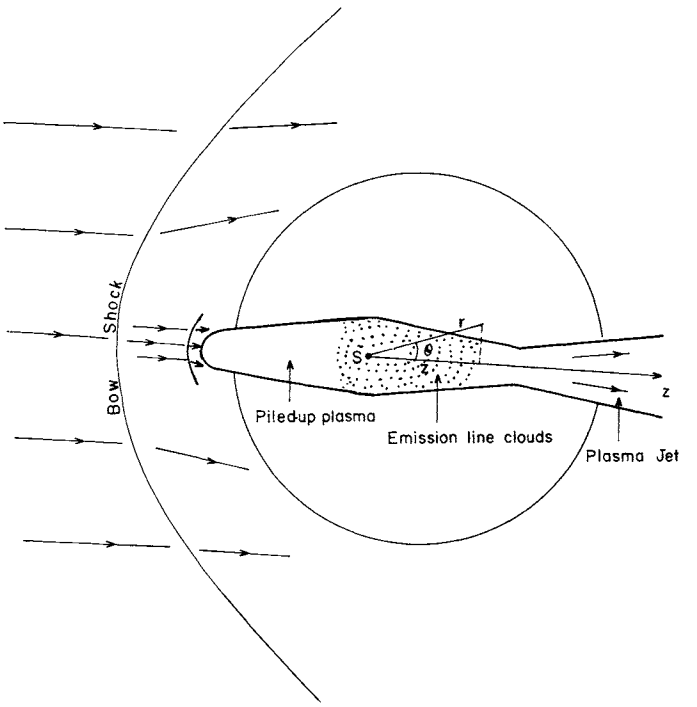

FIG. 2.—The steady state situation obtained in case B when the intergalactic medium is stopped by the gas cloud in a bow shock. Note that the forward jet has been stopped outside the gas cloud. The emission-line clouds are prevented from entering into the forward portion of the jet by the piled up plasma.

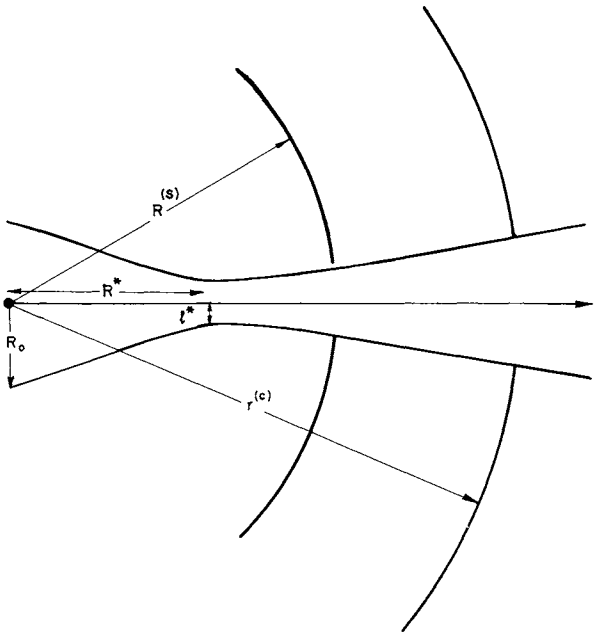

FIG. 3*a*

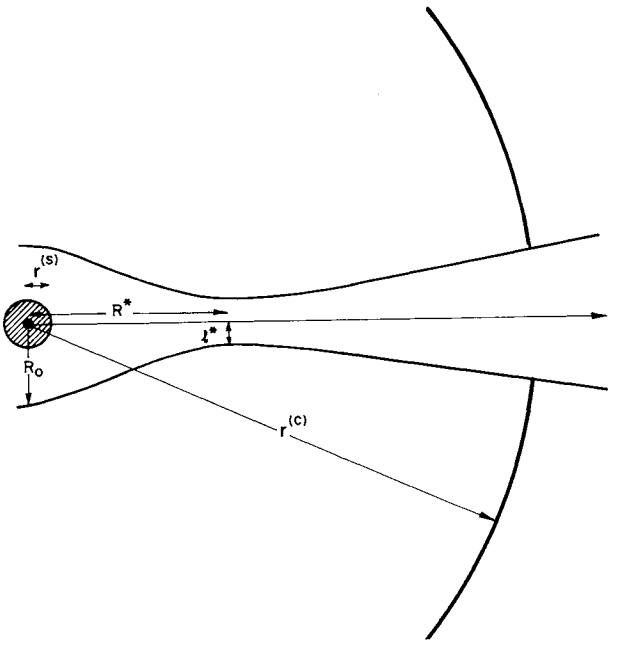

FIG. 3*b*

FIG. 3.—(*a*) The parameters of the jet mentioned in the text for type I distribution are shown here. The matter distribution extends up to a radius $R^{(s)}$, while the cloud extends up to $r^{(c)}$. (Figure not drawn to scale.) (*b*) The figure displays the parameters of the jet for type II distribution. The shaded region is the central massive object. (Figure not drawn to scale.)

Setting $p_0 \approx P^{(I)}$ and using equation (18) we get the above relation in the form $l^* = l_{pc}{}^*$ parsecs where

$$l_{pc}{}^* \approx 2.26\left(\frac{L_{41}}{n_{-5}{}^{(I)}}\right)^{1/2}(\gamma^2 - 1)^{-1/2} . \tag{20}$$

After passing through the de Laval nozzle, the plasma becomes supersonic. For relativistic plasma the bulk velocity at the nozzle is $c/\sqrt{3}$, and the nozzle is formed at a distance R^* where the pressure drops to four-ninths of its original value. Only exact fluid dynamical calculations will give the value of R^*. BR assumed $R^* \gtrsim 10l^*$ largely on the grounds that the jet is a linear structure. Numerical calculations of nonrelativistic plasma jets by Norman *et al.* (1981) indicate a compact fat jet with $R^* \sim 2l^*$ rather than a long and thin one. For our relativistic plasma the ratio R^*/l^* may lie somewhere in between (P. J. Wiita 1982, private communication). We therefore take $R^* \sim 4l^*$ while still retaining the analytic expressions of BR in most cases.

In the BR model, there is another parameter R_0 which characterizes the size of the central cavity from which the jet issues. The plasma issuing from the center expands spherically up to $\sim R_0$ and thereafter forms into the linear structure of a jet. BR determined the length R_0 by the requirement that at a distance of $2R_0$ from the center the jet radius is $R_0/2$. We will follow the same criterion.

a) Type I Distribution

In this case we use equation (8) and determine R^* by setting $r = R^*$ and $p = 4p_0/9$. This gives

$$R^* = \left(\ln\frac{9}{4}\frac{3kT}{\pi G\rho^{(s)}m_p}\right)^{1/2}$$
$$\approx 32\left(\frac{T_6}{\rho_{-19}{}^{(s)}}\right)^{1/2} \text{pc} . \tag{21}$$

The ratio $T_6/\rho_{-19}{}^{(s)}$ can be determined from equations (20) and (21) by requiring that $R^* = 4l^*$. Note that if T is fixed, $\rho^{(s)}$ is also known. We then have the following constraints on the radius $r^{(c)}$ of the cloud: $R^{(c)} > r^{(c)} > R^*$, indicating that the cloud is large enough to form the nozzle and small enough not to be blown apart.

Assuming a uniform matter distribution throughout the cloud its mass is given by

$$M = \frac{4\pi}{3}\rho^{(s)}r^{(c)3} . \tag{22}$$

We denote by M^* the *minimum* mass needed to form a nozzle. This is given by equation (22) for $r^{(c)} = R^*$.

In a local hypothesis the quasars should not be very massive. A galaxy like M87 has a massive object at its nucleus of mass $5 \times 10^9\ M_\odot$ (Young *et al.* 1978 and Sargent *et al.* 1978). If we assume that galactic nuclei in the mass range 10^8–$10^{10}\ M_\odot$ are ejecting quasars, then to avoid a total disintegration of the parent nucleus the mass $M^{(s)}$ of a typical quasar should not exceed $\sim 10^7\ M_\odot$. This is a further constraint on our model. In terms of this mass limit it is convenient to define a radius $R^{(s)}$ by

$$M^{(s)} = \frac{4\pi}{3}\rho^{(s)}R^{(s)3} \approx 2 \times 10^7\ M_\odot . \tag{23}$$

The radius of our uniform distribution should not exceed $R^{(s)}$.

Table 1 lists the various parameter values for $n^{(I)} = 10^{-3}$ cm^{-3}, 10^{-4} cm^{-3}, and 10^{-5} cm^{-3} for type I distributions in cases A and B. It will be seen that the inequality $R^{(c)} > R^*$ is *not* satisfied for case B for $n^{(I)} = 10^{-5}$ cm^{-3} unless $\gamma^2 - 1$ is fairly large. This would suggest that the transient effects of the IGM would blow off the cloud without forming a nozzle. The mass $M^{(s)}$ for case B has been determined for $R^{(s)} = R^{(c)}$. The quantity R_0 listed in Table 1 is calculated by using BR equation (3.2).

Table 1 also lists the relativistic γ-factor of the plasma by the time it leaves the confining gas cloud. Assuming that radiation from the plasma does not reduce γ_j in the jet significantly, the pressure in the jet falls as

$$p = p_0\gamma_j{}^{-4} . \tag{24}$$

The values given in Table 1 have been computed using equations (12) and (24) for $r = R^{(s)}$ and $r = \infty$. We note with BR that if the protons were initially injected with a γ-factor γ_0 then the bulk γ-factor will not increase much more than this value since the protons will become nonrelativistic at this stage.

TABLE 1

PHYSICAL PARAMETERS FOR TYPE I DISTRIBUTION

$n^{(I)}$	10^{-5} cm^{-3}	10^{-4} cm^{-3}	10^{-3} cm^{-3}
P_0 (dynes cm^{-2})	$1.5 \times 10^{-8}(\gamma^2 - 1)$	$1.5 \times 10^{-7}(\gamma^2 - 1)$	$1.5 \times 10^{-6}(\gamma^2 - 1)$
l^* (pc)	$2.26/(\gamma^2 - 1)^{1/2}$	$0.715/(\gamma^2 - 1)^{1/2}$	$0.226/(\gamma^2 - 1)^{1/2}$
R^* (pc)	$9.04/(\gamma^2 - 1)^{1/2}$	$2.86/(\gamma^2 - 1)^{1/2}$	$0.904/(\gamma^2 - 1)^{1/2}$
R_0 (pc)	3.43	1.08	0.343
T_6 (K)	0.3	0.3	0.3
M^*	$1.6 \times 10^7\ M_\odot$	$5 \times 10^6\ M_\odot$	$1.6 \times 10^6\ M_\odot$
$n_0^{(c)}$ (cm^{-3})	1.9×10^2	1.9×10^3	1.9×10^4
Case A: K/K_A	$8.9 \times 10^{-3}(\gamma^2 - 1)^{1/2}$	$2.7 \times 10^{-2}(\gamma^2 - 1)^{1/2}$	$8.5 \times 10^{-2}(\gamma^2 - 1)^{1/2}$
Case B: K/K_B	...	$2 \times 10^{-3}(\gamma^2 - 1)^{1/2}$	$10^{-3}(\gamma^2 - 1)^{1/2}$

	10^{-5} cm^{-3}		10^{-4} cm^{-3}		10^{-3} cm^{-3}	
$n^{(I)}$	Case A	Case B	Case A	Case B	Case A	Case B
$R^{(c)}$ (pc)	226	8.4	58	~ 3.9	18.4	~ 1.57
$R^{(s)}$ (pc)	9.8	...	4.54	3.9	2.11	1.57
$M^{(s)}$	$2 \times 10^7\ M_\odot$	...	$2 \times 10^7\ M_\odot$	$9.8 \times 10^6\ M_\odot$	$2 \times 10^7\ M_\odot$	$8.3 \times 10^6\ M_\odot$
$\gamma_j(R^{(s)})$	1.26	...	1.67	1.46	3.04	1.84
$\gamma_j(\infty)$	2.04	...	4.65	...	27.5	...

b) *Type II Distribution*

In this case we determine R^* using equation (10) for pressure. Writing $\mu = R^*/r^{(s)}$ and using the condition $p(R^*) = 4p_s/9$ we find that

$$\frac{\mu}{\mu - 1} = \ln\left(\frac{9}{4}\right)\frac{l}{r^{(s)}}\,. \tag{25}$$

We also have in this case,

$$R_0 \approx 2.6l^*\,, \qquad R^* = 4l^* + r_s \tag{26}$$

$$r_s = \frac{4l^*}{\mu - 1}\,. \tag{27}$$

Since we have assumed implicitly that $r_s < R_0$, we see from a comparison of equations (26) and (27) that $\mu \gtrsim 2.5$. We have taken $\mu = 3$ to work out the various parameters listed in Table 2 for case A only. (The inequality $R^{(c)} > R^*$ cannot be satisfied for case B, showing that the transient effects blow away the cloud before a nozzle could form.) Note that $\gamma_j(\infty)$ is not as high for the present type of matter distribution as it was for type I.

The values listed in Tables 1 and 2 for the various cases do satisfy the numerous constraints discussed earlier.

V. CONTINUUM EMISSION

Having discussed the gasdynamics of the cloud and the jet we now come to the radiation from the object. We discuss radiation in two forms, continuum radiation in this section and line radiation in the next.

We first note that in the rest frame of the quasar there is an inherent anisotropy. We have a backward jet through which plasma moves out relativistically. The velocity of the plasma at the nozzle is $c/\sqrt{3}$ corresponding

TABLE 2

PHYSICAL PARAMETERS FOR TYPE II DISTRIBUTION

$n^{(I)}$	10^{-5} cm^{-3}	10^{-4} cm^{-3}	10^{-3} cm^{-3}
μ	3	3	3
l^* (pc)	$2.26/(\gamma^2 - 1)^{1/2}$	$0.715/(\gamma^2 - 1)^{1/2}$	$0.226/(\gamma^2 - 1)^{1/2}$
$r^{(s)}$ (pc)	$4.52/(\gamma^2 - 1)^{1/2}$	$1.43/(\gamma^2 - 1)^{1/2}$	$0.452/(\gamma^2 - 1)^{1/2}$
R^* (pc)	$13.56/(\gamma^2 - 1)^{1/2}$	$4.29/(\gamma^2 - 1)^{1/2}$	$1.36/(\gamma^2 - 1)^{1/2}$
T_6 (K)	0.3	0.3	0.3
M	$6 \times 10^6\ M_\odot$	$2 \times 10^6\ M_\odot$	$6 \times 10^5\ M_\odot$
R_0 (pc)	5.88	1.86	0.588
$(l/K_1)^{1/2}$	6.2×10^{-2}	1.2×10^{-1}	1.7×10^{-1}
$R^{(c)}$ (pc)	106	18.8	3.3
$\gamma_j(\infty)$	1.36	1.36	1.36

to $\gamma = 1.22$. After going out from the nozzle, γ increases further. If the jet is reponsible for continuum radiation, it will be predominantly backwards in the quasar's rest frame.

What is the likely mechanism of conversion of the high kinetic energy in the jet plasma to radiation? Bremsstrahlung requires too high a density of gas in the jet. The other alternatives are inverse Compton process and synchrotron emission, of which the latter seems the more likely in quasars in view of the observed polarization. We show that synchrotron emission can be successfully accommodated in our model. The inverse Compton process might be needed to explain the X-rays from quasars.

a) A Simplified Calculation

Suppose the observed luminosity L comes from a volume V of the jet so that the required emissivity is $\epsilon = L/V$. To estimate V we take a length d of the jet and multiply it by the cross section πl^{*2} at the nozzle. Then we get from equation (20)

$$\epsilon \approx 2 \times 10^{-16} L_{41} n_{-5}^{(I)} d_{\rm pc}^{-1} \text{ ergs cm}^{-3} \text{ s}^{-1} . \tag{28}$$

The power radiated by an electron with energy $E_{\rm GeV}$ (in units of GeV) in a magnetic field B_{-4} measured in units of 10^{-4} gauss is given by

$$P \approx 4.24 \times 10^{-27} E_{\rm GeV}^2 B_{-4}^2 \text{ ergs s}^{-1} , \tag{29}$$

where we have averaged over the pitch angle. The radiation is predominantly at the frequency

$$\nu \approx 1.7 \times 10^9 B_{-4} E_{\rm GeV}^2 \text{ Hz} . \tag{30}$$

We estimate B_{-4} by the requirement that the magnetic pressure is small compared to the gas pressure:

$$\frac{B_{-4}^2}{8\pi} = \eta p_{-8} , \qquad \text{i.e., } B_{-4} = 5\eta^{1/2} p_{-8}^{1/2} , \tag{31}$$

where p_{-8} is the measure of p_0 in 10^{-8} dyne cm^{-2}, and η is small compared to 1. For optical or ultraviolet radiation ν is $\sim 10^{15}$ Hz. Expressing ν as ν_{15} in these units we get from expressions (29)–(31)

$$P \approx 1.25 \times 10^{-10} \eta^{1/2} \nu_{15} p_{-8}^{1/2} \text{ ergs s}^{-1} . \tag{32}$$

The number density of relativistic electrons needed to produce the required emissivity (28) is therefore

$$n_e \approx 1.6 \times 10^{-6} \eta^{-1/2} n_{-5}^{(I)} p_{-8}^{1/2} d_{\rm pc}^{-1} \text{ cm}^{-3} . \tag{33}$$

The γ-value of these electrons is $7 \times 10^5 \eta^{-1/4} p_{-8}^{-1/4}$, and their synchrotron lifetime is $\sim 130 \eta^{-3/4} p_{-8}^{-3/4}$ yr. Therefore in cases where p_{-8} is large, e.g., when $n^{(I)} = 10^{-3}$ cm^{-3} some *in situ* reacceleration may be needed.

b) Detailed Calculation

Having established the viability of synchrotron emission as a likely process for emission of continuum radiation, we now consider a more detailed picture. Suppose that the number density and spectrum of relativistic electrons at a distance r from the source of the jet is given by

$$d\bar{n}(r, \gamma_e) = n_0(r) \gamma_e^{-\beta} d\gamma_e , \qquad \beta = \text{constant} . \tag{34}$$

We assume that if necessary the electrons can be continuously accelerated within the jet. Blandford and Königl (1979) have suggested that particle acceleration in the jet can take place due to shocks associated with either dense clouds accelerated by the flow or with an unsteady velocity field in the jet. Let $\gamma_{\rm min} \leq \gamma_e \leq \gamma_{\rm max}$ and suppose that $\bar{n}(r)$ denotes the number density of relativistic electrons.

We will assume $\bar{n}(r)$ to be proportional to the number density $n(r)$ of relativistic plasma in the jet. From BR,

$$n(r) = \frac{4J}{L} p(r) \gamma_j(r) , \tag{35}$$

where J is the particle discharge and $\gamma_j(r)$ is the bulk γ-factor in the jet. J and L are constant along the jet. At the nozzle n is given by

$$n^* = \frac{8\sqrt{2}}{3\sqrt{3}} \frac{J}{L} p_0 . \tag{36}$$

We will assume that $\bar{n}(r) = \alpha n(r)$, α = constant. If $\tilde{\epsilon}$ is the energy per (e, p) pair ejected, then the number of electrons

ejected per unit time at the central source, J equals $L/\tilde{\epsilon}$. Expressing $\tilde{\epsilon}$ in GeV units, we get after a simple calculation

$$n_0(r) = 1.36 \times 10^{-5} \frac{\alpha p_{-8}(\beta - 1)\gamma_j^{*3}}{\epsilon_{\rm GeV}[\gamma_j(r)]^3} \{\gamma_{\rm min}^{1-\beta} - \gamma_{\rm max}^{1-\beta}\}^{-1} . \quad (37)$$

To compute the synchrotron spectrum we need $B(r)$, the magnetic field at r in the jet. Assuming that the field is disordered and that it scales inversely as the area of the jet, we determine it in terms of its value B^* at the nozzle. Assuming equation (31) to hold at the nozzle and using the relations given in the appendix to BR, we get

$$B(r) = \frac{(\gamma_j - 1)^{1/2}}{\gamma_j^3} \eta^{1/2} p^* . \quad (38)$$

Knowing the magnetic field and the energy distribution of electrons, it is now possible to calculate the total power emitted by a section of the jet between r_1 and r_2. Taking $\beta = 2$ for illustrative purposes we express the answer in the following form:

$$\mathscr{L} = 1.7 \times 10^{35} \alpha \nu_{15}^{1/2} \nu_{\rm min} \nu^{3/4} n_{-5}^{(I)3/4} L_{41} x(r_1, r_2) \text{ ergs s}^{-1} , \quad (39)$$

where r_1, r_2 are measured in parsecs and

$$x(r_1, r_2) = \int_{r_1}^{r_2} \frac{3\sqrt{3}}{2\sqrt{2}} \left[\frac{3\sqrt{3}(\gamma_j^2 - 1)^{1/2}}{2\gamma_j^3}\right]^{1/2} \gamma_j^{-2} dr . \quad (40)$$

The constant α is expected to be of order unity. $\gamma_{\rm min}$ may be as high as 10^3. A jet length of order 150 pc with $\eta = \frac{1}{5}$ and $n^{(I)} = 10^{-5}$ cm^{-3} gives an optical luminosity of $\sim 10^{40}$ ergs s^{-1}. For the larger value of $\gamma_{\rm min} \simeq 5 \times 10^4$ a smaller jet of 30 pc length can produce an optical luminosity of $\sim 10^{41}$ ergs s^{-1}. For larger $n^{(I)}$ the jet size is reduced.

At radio frequencies the power emitted by the same region is much smaller. Hence a correspondingly larger emitting volume is needed, unless a beaming effect mentioned below operates. This may explain why $< 10\%$ of all quasars are radio sources and why the radio emission comes from an extended volume.

The beaming effect comes from the anisotropy mentioned in the beginning of this section. If we consider the radiation pattern in the quasar's rest frame then the radiation emitted by plasma with bulk velocity V_j in the forward direction exceeds that in the backward direction of motion of the plasma by the factor

$$\lambda = \left(\frac{c + V_j}{c - V_j}\right)^{2.5} . \quad (41)$$

As $V_j \sim V_j^* = c/\sqrt{3}$, this value is ~ 27. It will be even higher for plasma which has passed through the nozzle. Thus, if we happen to be aligned along the forward direction of the jet (i.e., the backward direction of the quasar), the quasar will appear brighter. This may be why radio quasars are comparatively rare.

Because of this beaming effect, in a flux limited sample, those quasars will predominate for which the observer is located in the backward direction. Such quasars tend to be redshifted. An effect of this type was quantitatively discussed in Paper I. It is, however, necessary to look at line emission also since spectral shift is measured for lines rather than the continuum.

VI. LINE EMISSION

a) Location and Mass of a Line-Emitting Region

The mass of the emission-line regions in quasars can be estimated in terms of line intensities, electron number density N_e, and electron temperature T_e (Burbidge and Burbidge 1967). The estimates of N_e and T_e are independent of whether quasars are local or distant and are usually in the range $10^{8.5} \lesssim N_e \lesssim 10^{9.5}$ cm^{-3} and $T_e \sim 10^4$ K (Davidson and Netzer 1979; Veron 1979). Using the Hβ luminosity, the mass of the line emitting region is given by (cf. Veron 1979)

$$M_E = 85 x^{-1} L_{43}(\text{H}\beta) N_{e9}^{-1} M_\odot , \quad (42)$$

where $x(N_e, T_e)$ lies in the range $0.17 < x < 3.71$ but is usually close to 1 (Krolik and McKee 1978). For $x \sim 1$ and an Hβ luminosity (scaled down for local quasars by a factor of 10^4) of $\sim 10^{39}$ ergs s^{-1}, we get $M_E \sim 10^{-2} M_\odot$. This value is several orders of magnitude smaller than the overall mass of the system as given in the various models of Tables 1 and 2. Thus the line emitting regions do not affect the overall dynamics of the system, and they can be placed anywhere in the composite system, without affecting our previous considerations.

If the filling factor of the line emitting region were unity, then the radius of the line emitting gas of mass $M_E \sim 10^{-2} M_\odot$, and $N_e \sim 10^9$ cm^{-3} would be $\sim 5 \times 10^{-4}$ pc. If the filling factor were as small as 10^{-6}, this radius would increase only to 5×10^{-2} pc. These small values suggest that the emission line gas cloud could be placed

within the central cavity or in the jet. We could imagine $\sim 10^4$ such clouds, each of mass $\sim 10^{-6}\ M_\odot$ coexisting with relativistic plasma at higher temperature. Such clouds appear to be of small enough mass to be thought of as ejecta from the central source. From considerations of the following subsection, we would expect the clouds to be mainly in the jet, although not too far from the central cavity. The following scenario may be offered by way of explaining their location in this part of the object.

There are three forces acting on a typical emission line cloud. The first is the inward gravitational pull of the mass distribution (of type I or II). The second is the ram pressure force of the plasma in the jet flowing past the cloud, while the third is the force caused by the pressure gradient in the jet. Numerical estimates show that for the values quoted in Tables 1 and 2, the gravitational attraction dominates over the other two forces up to a characteristic distance D, for which an escape speed V_D can be computed. For an initial ejection speed $v \leq V_D$, the clouds reach a maximum distance D and fall back to the center, while for $v > V_D$, the clouds escape from the object altogether. It should be noted at this stage that while in case A models the ejected clouds can travel only in the backward jet, in case B models, some clouds may be ejected in the forward direction. However, these clouds are prevented from traveling far in this region by the piled up plasma there and by the pressure gradients due to the ram pressure of the IGM.

For a local quasar moving relativistically, the travel time across a galactic distance of ~ 30 kpc is $\sim 10^5$ yr. This is comparable to the time taken by a cloud of ejection speed V_D to travel a distance D. Thus, at the time of observation the fast moving clouds ($v > V_D$) would have left the quasar, and only those trapped within $r \leq D$ would be seen.

b) The Resolution of Blueshift Catastrophe

We now come to the basic question: why blueshifted lines are not seen in the quasar spectra in the Doppler theory. In § V we noted the beaming effect of the continuum in the backward direction of quasar's motion. Quasars are usually spotted by their continuum emission in the visual range and sometimes through X-rays or radio waves. These selection procedures work against the detection of blueshifted quasars whose continuum emission will be lower. Nevertheless, once a blueshifted quasar is picked up, should not its line radiation reveal the blueshift? We show below that a small dust component in the surrounding cloud of the quasar is sufficient to prevent our seeing blueshifted lines.

We illustrate the scenario with Figure 4. As seen in § VI*a*, the line emitting clouds are assumed to exist in the jet in an off-center position. Consider a typical cloud located at point R (cf. Fig. 4), and let RF and RB be two

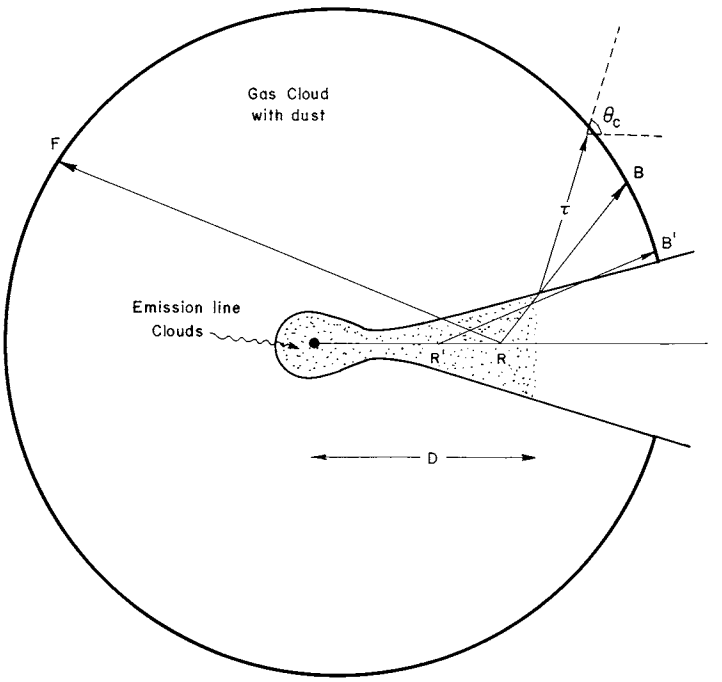

FIG. 4.—The figure illustrates how the problem of "blueshift catastrophe," mentioned in the text, is resolved. The optical depth of the cloud needed for absorption is $\sim\tau$. The emission-line clouds at R can be easily seen in the backward direction RB but cannot be seen along the direction of RF. R'B' is a path mentioned in the text which transverses the optically thin jet for some distance before encountering the cloud. The dotted line indicates a limiting direction θ_c. For angles greater than θ_c the line emitting clouds are obscured by the dust.

directions from R, one in the forward direction and the other in the backward direction. We wish to argue that in general RF will be long enough to block line radiation in the forward direction, while, RB being small, radiation escapes in the backward direction.

We will assume the dust in the form of spherical grains of graphite of radius $\sim 2.5 \times 10^{-6}$ cm and suppose that it accounts for a fraction f of the cloud by mass. The characteristic distance over which visual wavelengths are absorbed is then given by

$$\tau \sim (\kappa f n^{(c)} m_p)^{-1} \sim 2\kappa_5^{-1} (f n^{(c)})_0^{-1} \text{ pc} , \tag{43}$$

where κ_5 is mass absorption coefficient κ expressed in units of 10^5 cm^2 g^{-1} and $fn^{(c)}$ is expressed in (cm^{-3}). For models in Tables 1 and 2, $n^{(c)}$ ranges from 10^2 to 10^4 cm^{-3}. In the interstellar medium of our Galaxy, $f \sim 10^{-2}$ (Spitzer 1978). The presence of dust in quasars has been observationally established (Davidson and Netzer 1979) and the value $f \sim 10^{-3}$ in expression (43) does not seem excessive. Then even with $n^{(c)} \sim 10^2$ cm^{-3}, τ is as low as 20 pc. This is small compared to the characteristic cloud size in Tables 1 and 2.

It is worth pointing out in this connection that the characteristic optical depth for scattering by the gas in the cloud is about 10^3 times longer, so that gas by itself is not able to block blueshifted lines; dust is essential for the model to work. Note also that if the line emitting region is situated fairly close to the central region, *no* lines will be seen. For R in Figure 4 located within a distance τ from the periphery of the gas (+dust) cloud, lines will be seen in the backward direction only. Further, the presence of the jet in the backward direction enhances this effect by allowing light rays in this direction paths (like R′B′ in Fig. 4) which traverse the optically thin jet for some distance before encountering the gas cloud. This allows one to see more emission-line clouds for backward directions closer to the jet axis.

At this stage we note that the presence of dust does not diminish the optical continuum in the same way as it does the line emission. This is because the line emission is restricted to regions $r \leq D$, whereas the optical continuum originates from all along the jet.

We have investigated the survival conditions for dust in the gas cloud. Grains could in principle be destroyed (*a*) through sputtering of gas, (*b*) by heating due to radiation from the central cavity, and (*c*) by the heating due to collisions with the ambient gas. Besides, in case A, the IGM going through the cloud can disrupt the grains. None of these factors are significant for the parameters of our model.

VII. DISCUSSION

We have outlined a plausible model for a Doppler quasar whose radiation (both line and continuum) is predominantly backward. While we have explained why no blueshifts are likely to be seen, a more precise mathematical treatment is necessary to estimate the N_b/N_r ratio. Such a computation was done in Paper I for a specific class of anisotropic emission. If, as discussed in § VI*b*, the damping of lines is not complete outside the Hoyle angle, it will in principle be possible to see some blueshifted quasars. To this extent it is likely that some of the lines may have been misidentified in a few of the observed quasars.

In § VI*b* we also considered the possibility that no lines are seen when the line emitting region is situated well inside the confining cloud. Such objects will be seen as BL Lac objects. In the event of a line emitting region moving outwards, a BL Lac may be seen to change to a normal quasar.

We have already commented on the two observed features of radio quasars: (*i*) their comparatively large radio emitting regions, and (*ii*) their comparative rarity. Apart from these features, our model offers an explanation as to why in all the observed cases of quasars only one radio jet is seen. To explain the smaller fraction of doubles, we recall that in case B a weak jet might form in the forward direction and end up in a radio hot spot in the front also. We propose to investigate this effect and the formation of radio lobes in a later paper. By an extension of the reasoning given in § VI*a* we expect that the extra pressure gradients due to the IGM ram pressure would push the line emitting regions further inside. Thus the lines would be seen in the backward jet only.

In § III we found that the extent of the gas cloud surrounding the central object is determined by the IGM ram pressure and hence by the speed with which the quasar moves through the IGM. Quasars with large Doppler shift would have smaller clouds than quasars with small Doppler shift. If the cloud is seen as a fuzz around the central bright object, it is likely that the fuzz would be associated with low redshift quasars. The distance of the quasar from us is also important in determining the apparent angular size of the fuzz. Thus a cloud of 200 pc diameter at a distance of 10 Mpc will subtend an angle of 4″ at the observer. Systematic searches for fuzz around quasars will therefore provide a test for this model.

Some of the various parameters of the model can be scaled *up* to luminosities $\sim 10^{46}$ ergs s^{-1} for quasar models in the cosmological hypothesis. To avoid substantial Doppler components and yet have sufficient ram pressure from the IGM we need $V/c \lesssim 0.3$, say. The reduction of the IGM ram pressure may be compensated by higher values of $n^{(I)}$. Thus it may be possible to have viable models for $n^{(I)} = 10^{-3}$ cm^{-3}. Such models might well be needed to understand single jet quasars within the framework of the cosmological hypothesis.

A quasar moving with relativistic speed at a distance of ~ 100 Mpc will have a proper motion of the order 0.6 milli-arcsec per year. Improvements in VLBI techniques may be able to detect such proper motions in the future.

A positive effect would be a direct verification of the Doppler hypothesis, especially if the jet is in the backward direction.

One of us (J. V. N.) was at the Kitt Peak National Observatory when this work was started. He thanks Geoffrey Burbidge, David De Young, and Peter Strittmatter for critical comments in the initial stages. We have also received considerable help from discussions with Paul Wiita in the final stages of this work.

REFERENCES

Arp, H. 1967, *Ap. J.*, **148**, 321.
———. 1977, in *IAU Colloquium 37, Decalages vers le Rouge et Expansion de l'Univers*, ed. C. Balkowski and B. E. Westerlund (Paris: C.N.R.S.), p. 377.
Arp, H., and Hazard, C. 1980, *Ap. J.*, **240**, 726.
Blandford, R. D., and Königl, A. 1979, *Ap. J.*, **232**, 34.
Blandford, R. D., and Rees, M. J. 1974, *M.N.R.A.S.*, **164**, 395 (BR).
Burbidge, G. R. 1973, *Nature*, **246**, 17.
———. 1979, *Nature*, **282**, 451.
Burbidge, G. R., and Burbidge, E. M. 1967, *Quasi-stellar Objects* (San Francisco: Freeman).
Davidson, K., and Netzer, H. 1979, *Rev. Mod. Phys.*, **51**, 715.
Fabian, A. C., and Kembhavi, A. K. 1982, in *IAU Symposium 97, Extragalactic Radio Sources*, ed. D. S. Heeschen and C. M. Wade (Dordrecht: Reidel), p. 453.
Field, G. B. 1972, *Ann. Rev. Astr. Ap.*, **10**, 227.
Field, G. B., Arp, H., and Bahcall, J. N. 1973, *The Redshift Controversy* (London: Benjamin).
Henriksen, R. N., Vallée, J. P., and Bridle, A. H. 1981, *Ap. J.*, **249**, 40.
Hoyle, F. 1980, Astrophysics and Relativity preprint 63 (University College, Cardiff).
Hoyle, F., and Burbidge, G. R. 1966, *Ap. J.*, **144**, 534.
Icke, V. 1983, *Ap. J.*, **265**, 648.
Jones, T. W., and Owen, F. N. 1979, *Ap. J.*, **234**, 818.
Krolik, J. H., and McKee, C. F. 1978, *Ap. J. Suppl.*, **37**, 459.
Lea, S. M., and De Young, D. S. 1976, *Ap. J.*, **210**, 647.
Narlikar, J. V., and Subramanian, K. 1982, *Ap. J.*, **260**, 469 (Paper I).
Norman, M. L., Smarr, L., Wilson, J. R., and Smith, M. D. 1981, *Ap. J.*, **247**, 52.
Rees, M. J. 1977, in *IAU Colloquium 37, Decalages vers le Rouge et Expansion de l'Univers*, ed. C. Balkowski and B. E. Westerlund (Paris: C.N.R.S.), p. 563.
Rudermann, M. A., and Spiegel, E. A. 1971, *Ap. J.*, **165**, 1.
Sargent, W. L. W., Young, P. J., Boksenberg, A., Shortridge, K., Lynds, C. R., and Hartwick, F. D. A. 1978, *Ap. J.*, **221**, 731.
Spitzer, L. 1978, *Physical Processes in the Interstellar Medium* (New York: Wiley-Interscience).
Strittmatter, P. 1967, cited in *Quasi-stellar Objects* by Burbidge, G. R., and Burbidge, E. M. (San Francisco: Freeman), p. 164.
Terrell, J. 1964, *Science*, **145**, 918.
Veron, P. 1979, in *Physical Cosmology, Les Houches Session XX*, XII (Amsterdam: North-Holland), p. 311.
Wiita, P. J., and Siah, M. J. 1981, *Ap. J.*, **243**, 710.
Young, P. J., Westphal, J. A., Kristian, J., Wilson, C. P., and Landauer, F. P. 1978, *Ap. J.*, **221**, 721.

J. V. NARLIKAR and K. SUBRAMANIAN: Theoretical Astrophysics Group, Tata Institute of Fundamental Research, Homi Bhabha Road, Bombay 400 005, India